Article

Characterization of Micro-threaded Stem Taper Surface of Cementless Hip Endoprostheses

Drago Dolinar , Boštjan Kocjančič , Klemen Avsec , Barbara Šetina Batič , Aleksandra Kocijan , Matjaz Godec , Mojca Debeljak , John T Grant , Timon Zupanc , Monika Jenko *

Posted Date: 13 May 2024

doi: 10.20944/preprints202405.0688.v1

Keywords: total hip arthroplasty; stem micro-threaded taper; taper surface morphology , microstructure , corrosion; Ti implant alloy

Article

Characterization of Micro-Threaded Stem Taper Surface of Cementless Hip Endoprostheses

Drago Dolinar [1,2], Boštjan Kocjančič [1,2], Klemen Avsec [1], Barbara Šetina Batič [3], Aleksandra Kocijan [3], Matjaž Godec [3], Mojca Debeljak [4], John T Grant [5], Timon Zupanc [1] and Monika Jenko [6,7,*]

[1] Dept. for Orthopaedic Surgery, University Medical Centre Ljubljana, Zaloška 9 , 1000 Ljubljana, Slovenia, dolinardrago@gmail.com, kocjancicb@gmail.com, timon.zupanc@gmail.com
[2] Faculty of Medicine, University of Ljubljana, Vrazov trg 2, 1000 Ljubljana, Slovenia
[3] Institute of Metals and Technology, Lepi pot 11, 1000 Ljubljana, Slovenia; barbara.setina@imt.si, Aleksandra.kocijan@imt.si
[4] University Rehabilitation Institute Republic of Slovenia, Linhartova 51, 1000 Ljubljana, Slovenia, mojca.debeljak@ir-rs.si
[5] Research Institute, University of Dayton, Dayton, OH 45469, USA; john.grant@surfaceanalysis.org
[6] MD-RI Institute for Materials Research in Medicine, Bohoričeva 5, 1000 Ljubljana, Slovenia monica.jenko@gmail.com
[7] MD Medicina, Sanatorium, Bohoričeva 5a, 1000 Ljubljana, Slovenia
* Correspondence: monika.jenko@imt.si, +386 31 311 076

Abstract: We investigated micro-threaded stem taper surface and the impact on premature failures, aseptic loosening, and infection. We have focused on the fretting, and crevice corrosion of micro-threaded tapers, as well as the characterization of microstructure and surface properties of two new and three retrieved Zweymüller stem tapers of cementless hip endoprostheses selected from a set of 45 stems. The retrievals examined were those in which the sole source of modularity with a metallic component was the head-stem taper interface between the Ti alloy taper stem and the ceramic head. To determine the surface chemistry and microstructures of both new and retrieved hip endoprostheses stem taper titanium alloy, scanning electron microscopy (SEM) was employed for morphological and microstructural analyses. At the same time, energy dispersive spectroscopy (EDS) was utilized for characterizing chemical element distribution, and electron backscattered diffraction (EBSD) was used for phase analysis. The micro-threated stem taper's roughness for different manufacturers was investigated using an optical profilometer. Standard roughness parameters Ra (average surface roughness) and Rz (mean peak to valley height of the roughness profile) were used in this investigation. Additionally, profile depth and peak spacing for different samples were investigated. The surface roughness results indicate no significant difference in roughness associated with varying survivorship times, ranging from 3 to 239 months, and across different manufacturers. Electrochemical studies revealed no fretting corrosion in retrieved stem tapers (ceramic head) that prematurely failed due to aseptic loosening after 239 months, infection after 3 months, and low-grade infection after a 32-month lifetime. Therefore, three retrieved tapers and two new ones for comparison underwent potentiodynamic measurements in Hank's solution to ascertain the corrosion rate of new and retrieved stem taper surfaces. The results show a low corrosion rate for both new and retrieved samples that failed prematurely due to aseptic loosening. However, the corrosion rate of infected and low-grade infected tapers was higher. In conclusion, our study aligns with existing literature, suggesting that the use of ceramic heads decreases the problem of taper corrosion and subsequently reduces premature failures in total hip arthroplasty.

Keywords: total hip arthroplasty 1; stem micro-threaded taper 2; taper surface morphology 3; microstructure 4; corrosion 5; Ti implant alloy 6

 doi:10.20944/preprints202405.0688.v1

1. Introduction

Total hip arthroplasty (THA) replacement surgeries have been very successful for decades. Kurtz et al. reported that the number of patients in the USA who need a THA and consequent revision is increasing because of an aging population [1].

The fixation of the metal and later ceramic head to the titanium alloy stem is achieved by a Morse taper, which consists of a stem taper (male taper) and a taper in the femoral head (female taper) [2–4]. Each stem taper has characteristic properties such as taper angle, diameter, base dimension, straightness, roundness, and surface properties, as shown in Figure 1. Every modular connection of metal alloys in contact with body fluids and exposed to micromotion is subject to corrosion [5–7]. The taper's interface is influenced by several factors, such as (i) design and material, (ii) assembly (surgical factors), and (iii) loading (patient factors) [3,6]. Urish et al. explained in detail the basic principles of corrosion types that can occur in an orthopedic implant surface including pitting, crevice, fretting, and mechanically assisted crevice corrosion [6].

Figure 1. The measured taper characteristics are proximal female and distal male diameters, contact length, and total length, as shown for a stem taper at the left. The investigated cementless hip stems from different manufacturers. 1-SL-Plus, Smith & Nephew, 2-Alloclassic Varial Zimmer, 3-Alloclassic Zweymüller Zimmer, 4-Adler Ortho Modula, and 5- Lima corporate ZM C2.

Cales et al. reported that each implant company applies its specifications for manufacturing and discussed the advantages and disadvantages of standardization of tapers in hip endoprostheses [8]. However, until today, no uniform taper regarding dimensions, metallurgy, manufacturing tolerances, or surface finish has been achieved by the International Organization for Standardization (ISO) and ASTM International [8]. The general standard is 12/14 (it was pioneered in the orthopedic industry by the Italian firm Cremascoli, formerly known as Adler Ortho), indicating a 12 mm diameter at the apex of the cone and 14 mm at its base. However, the exact length of the taper is not rigorously defined, thus the angle may exhibit slight variations. It is recommended, particularly for partial dentures, that both components originate from the same manufacturer. However, this recommendation becomes less imperative during revisions, where strict adherence is not maintained. The specific shape of the taper, including notches and surface finish, remains undefined.

Approximately 60 different types of cementless stem components [17] of hip prostheses are currently available on the market and knowledge of the behavior of the individual prosthesis in certain clinical conditions is very important [6,9–19].

The Zweymüller cementless hip endoprosthesis with SL-PLUS® femoral stem has been used for the last 30 years with no change in design. It is made of forged titanium Ti6Al7Nb alloy, or in the USA and non-EU countries Ti6Al4V alloy, with a double-taper straight stem of rectangular cross-section. Its grit-blasted 2-5 μm surface roughness enhances bone ingrowth. Roškar et al., report that till now, there has been no report on more than 2000 Zweymüller endoprostheses from a single center with over 20 years of follow-up [20,21].

Aseptic loosening and periprosthetic joint infection are the main causes of the premature failure of joint arthroplasty [12,15]. Aseptic loosening can be induced by different causes, such as the micromotion of the implant in the bone during loading, corundum wear particles from grit-blasted

 doi:10.20944/preprints202405.0688.v1

surfaces, including taper, wear-particle generation, causing inflammation and bone resorption, and consequently the formation of a poor functional interface (osteointegration) between the implant and the patient's bone [22–27].

The aim of the present study is the investigation of cementless Zweymüller stems, the femoral component, of hip endoprostheses. We were interested in the micro-threaded stem taper and its influence on premature failure, aseptic loosening, and infection. We have focused on the characterization of surface properties, micromorphology, microstructure, phase structure, and surface properties of two new (Alloclasic of Ti6Al7Nb and Lima Corporate of Ti6Al4V alloy) and three retrieved taper stems.

We examined retrievals in which the only source of modularity with a metallic component was the head-stem interface between the Ti6Al7Nb alloy taper stem and the ceramic head.

Stockhausen et al. reported that the degradation at the modular head-neck interface in THA is predominately expressed in the form of corrosion and fretting, potentially causing peri-prosthetic failure by adverse reactions to metal debris [2]. Their retrieval study aimed to quantify variations in stem taper surface topographies and to assess the influence on the formation of corrosion and/or fretting in titanium alloy stem tapers combined with ceramic heads. They found high variability in surface characteristics between threaded stem tapers: Alloclassic and CLS tapers feature deeply threaded trapezoid-shaped profiles with thread heights over 65 μm; low thread heights below 14 μm characterize the sawtooth-shaped Bicontact and triangular SL-Plus taper. Significantly lower corrosion and fretting scores were observed in lightly threaded, compared to deeply threaded, tapers in ceramic head combinations. They concluded that the relationship between stem taper surface topography and the formation of clinical results of corrosion and fretting could help improve the performance of modern THAs and lead to longer-lasting clinical results [2,3,28,29].

The aim of this study is the characterization of microstructure, surface properties, and microtopography of new and retrieved 12/14 stem tapers of different manufacturers where the retrievals examined were those in which the sole source of modularity with a metallic component was the head-stem taper interface between the Ti alloy taper stem and the ceramic head.

2. Materials and Methods

2.1. Materials

All the retrieved Ti6Al7Nb stems of the cementless Zweimüller (ZM) type hip endoprostheses were collected within the frame of the register of the explanted orthopaedic endoprostheses (UMC-Ljubljana, Slovenia) during the revision surgeries. For comparison, we investigated two out of five new stems (after their expiry date) of Smith & Nephew, Alloclasic Varial, Alloclasic Zimmer, and Lima Corporate manufacturers. The investigation included 45 stems of cementless hip endoprostheses that prematurely failed due to (i) aseptic loosening (15 implants), (ii) infection (15 implants), and (iii) low-grade infection (15 implants). The interval between the primary hip replacement and the revision surgery was 36 months to 259 months for aseptic loosening, 3 months to 40 months for infection, and 12 months to 198 months for low-grade infection [3,13,14].

The retrieved stems were SL-Plus, Smith & Nephew (London UK), and Endoplus (London, UK) manufacturers. The retrieved implants were sent after the revision surgery for sonication and microbiological analyses in Ringer's solution and afterward for cleaning and sterilization [3–6].

The samples: tapers, described in Table 1, and in Figure 2, were cut from the stems, and cleaned by standard procedures. The micro-threaded taper surface of 5 selected samples: (i) A-283-239 month -aseptic loosening, (ii) I-212-32 month- infection, (iii) I -129-32 low-grade infection, (iv) Alloclassic Varial -new and (v) Lima Corporate-new (Ti6Al4V), were examined.

 doi:10.20944/preprints202405.0688.v1

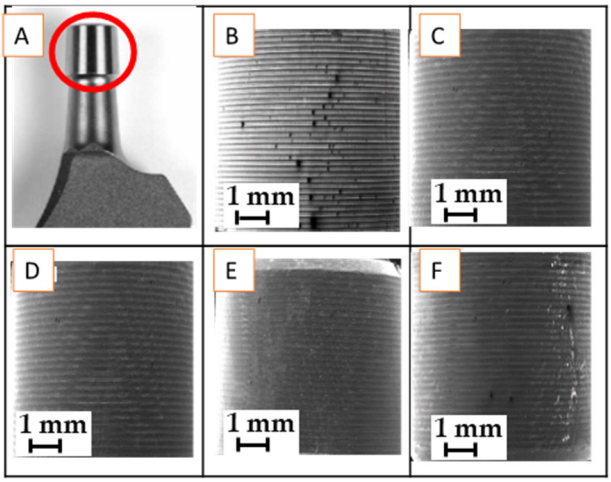

Figure 2. (A) micro threaded 12/14 stem taper, new Smith & Nephew, (B-F): 11x magnification SEM/SE images of different ZM 12/14 tapers and different manufacturers: (B) Alloclasic Varial new, (C) Lima new, (D) retrieved I-212-32-month, Smith & Nephew, (E) retrieved I-31-129-month, Smith & Nephew, and (F) retrieved A383-239 month, Endoplus.

Table 1. Investigated samples of new and retrieved stem tapers.

Number	Sample	Lifetime month	Cause of premature failure	Material	Tapers
1	Allocassic Varial	new		Ti6Al7Nb - ZM stem	12/14
2	Lima Corporate	new		Ti6Al4V - ZM stem	12/14
3	I-212	032	Infection	Ti6Al7Nb/ceramics BD- diameter 36**	12/14
4	I-031	129	Low-grade infection	Ti6Al7Nb/ceramics BD -diameter 32**	12/14
5	A-283	239	Aseptic loosening	Ti6Al7Nb/ceramics BF -diameter 32*	12/14

*Ceramic head Biolox Forte, BF; ** Ceramic head Biolox Delta, BD, ZM-ZweyMuller.

2.2. Methods

The morphology, microstructure, surface chemistry, and phase analysis of the samples of both Ti6Al7Nb and Ti6Al4V alloys, were investigated in the field-emission scanning electron microscope (ZEISS crossbeam 550 FIB-SEM Carl Zeiss AG, Oberkochen, Germany).

The instrument is equipped with secondary-electron (SE), backscattered-electron (BE) imaging modes for analyses of the morphology of the samples and energy-dispersive X-ray spectroscopy, EDS, (EDAX, Octane Elite, Draper, Cambridge, MA, USA) for the surface chemistry (to a depth of about 3 μm). For the SE and BE imaging an acceleration of 15 kV at a current of approximately 1.5 nA was used at a vacuum below 10^{-6} mbar.

For phase analysis and grain orientation, the instrument is equipped with an electron back-scattered diffraction analyzer, EBSD, with Hikari Super Plus camera with ApeX (Edax) software, and data analyzed in OIM (Edax).

The micro-threaded surface roughness of stem tapers was measured using the optical profilometer made by Alicona Infinite Focus G4 (Raaba-Grambach, Austria). Standard roughness parameters *Ra* - average surface roughness and *Rz* - mean peak to valley height of roughness profile were used for this investigation. Profile depth and peak spacing for different samples were also investigated. For all samples, the evaluation length was 2.67mm.

For corrosion rate measurement, an electrochemical study was performed in a simulated physiological Hank's solution at 37 °C and pH = 7.8 using a BioLogic Modular Research Grade

 doi:10.20944/preprints202405.0688.v1

Potentiostat/Galvanostat/FRA Model SP-300 (BioLogic Science Instruments, Seyssinet-Pariset, France) with EC-Lab Software (EC-Lab V11.27). The experiments were carried out in a three-electrode cell where tested specimens were employed as the working electrode (WE), a saturated calomel electrode (SCE, 0.242 V vs. SHE) as the reference electrode (RE), and a platinum net as the counter electrode (CE). The samples were stabilized at the open-circuit potential (OCP) for 1 h before the electrochemical measurements were made. The potentiodynamic curves were measured with a scan rate of 1 mV s^{-1} from -250 mV vs. SCE according to the OCP [30].

All the measurements were repeated three times.

3. Results

3.1. Microstructure of Ti6Al7Nb and Ti6Al4V Stem Tapers

The microstructure of the stem taper of the implants manufactured from Ti alloys (Ti6Al7Nb and Ti6Al4V) is shown in Figure 3. A dual-phase microstructure is observed in the matrix, Ti phase is α -Ti (dark grey) and the Nb-rich or V-rich phase (light grey) is β-Ti (Figure 4). The dual-phase structure is confirmed using the EBSD method (Figure 5).

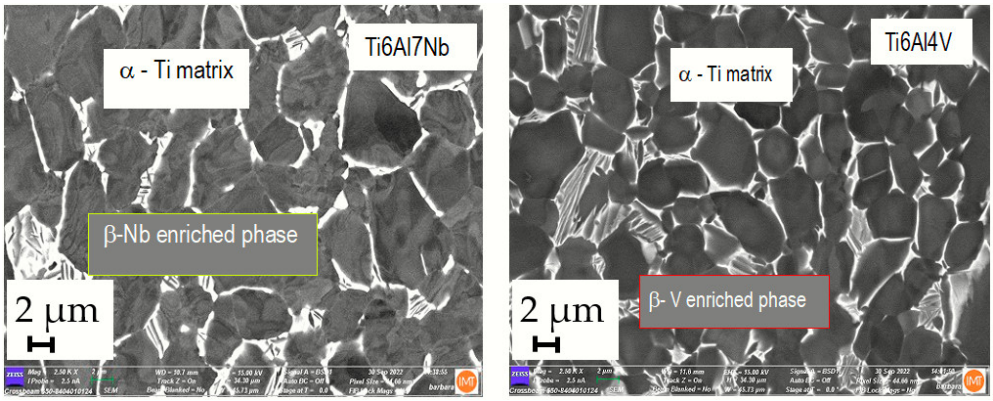

Figure 3. SEM/BE image of Ti6Al7Nb alloy microstructure (A283). It consists of two phases (α+ β). α -phase (dark) represents the matrix which has a close-packed hexagonal crystal structure (hcp), and the β -Nb-enriched β phase (white) in the body-centered cubic structure. (b) SEM/BE image of Ti6Al4V alloy microstructure of new Lima stem. α -phase (dark) represents the matrix, β phase V-enriched phase (white) at M2500.

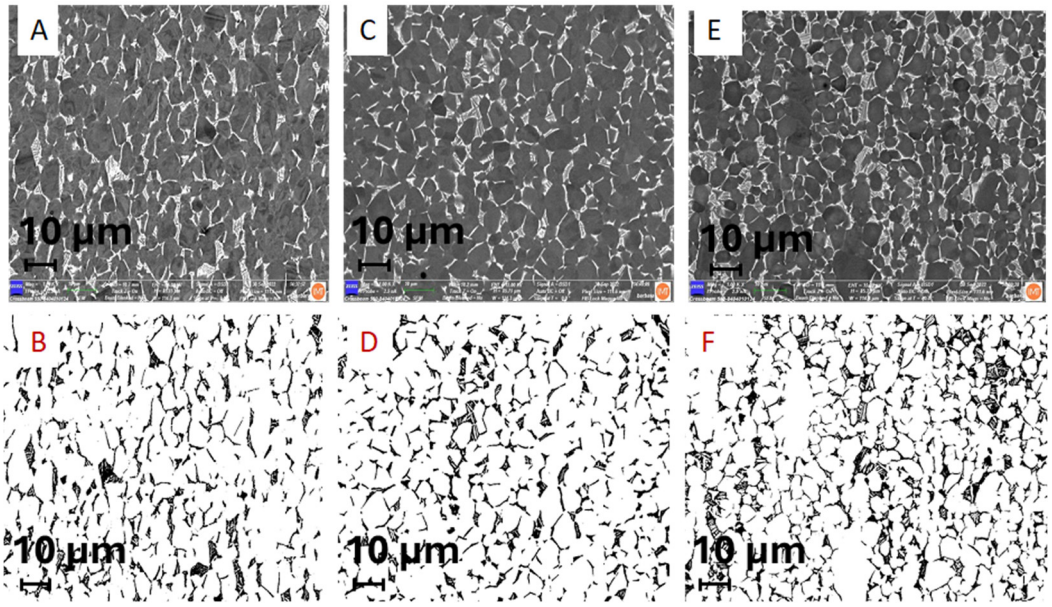

 doi:10.20944/preprints202405.0688.v1

Figure 4. (A-B) BE/SE image of dual phase microstructure (α + β) and their distribution of a stem taper retrieved after 239 months (ENDOPLUS, London, UK) prematurely failed due to aseptic loosening Ti6Al7Nb alloy A-283, M1000; (C-D) SEM/BE image of dual phase microstructure (α + β) and phase distribution in stem taper prematurely failed after 3 months due to infection, I-31 Smith & Nephew (London, UK), M1000, (E-F) SEM/BE image of dual phase microstructure α + β and their distribution of new stem taper Lima, made of Ti6Al4V alloy, M1000 β-phase in the row below(b, d, e) is black. The amount of α (Ti, Al, O, N, matrix) and β (Nb or V enriched phase) is represented in Table 2.

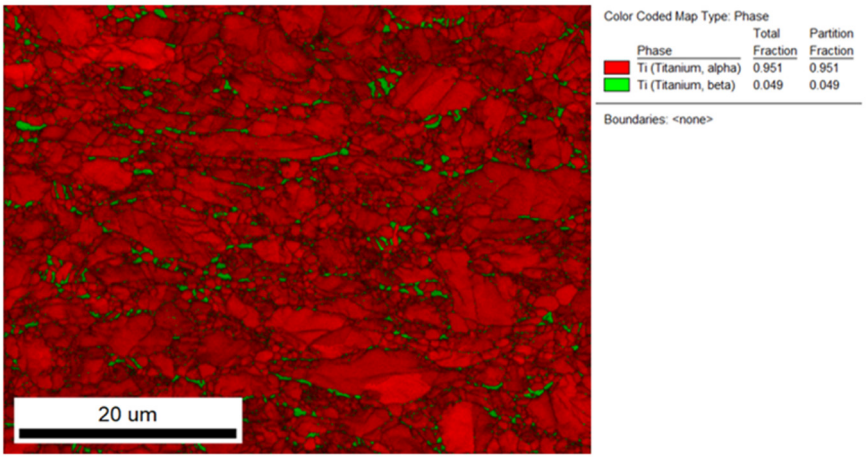

Figure 5. EBSD image of Ti6Al7Nb new sample. α phase is Ti matrix in hcp structure, red, and with Nb enriched β phase, bcc structure green.

Table 2. Microstructure analysis: the estimation of investigated stem tapers proportion of α and β phase.

SAMPLE No/ STEM TAPER ALLOY	Survivorship of THA /months	Magnif-ication	Analyzed area (μm²)	Content **α**-phase (%)	Content **β** -phase (%)
A 283 02/Ti6Al7Nb	239	250	143.05	85,32	14,68
A 283 04/Ti6Al7Nb	239	500	38.59	87,06	12,94
A 283 06/Ti6Al7Nb	239	1000	9.69	87,51	12,49
I 212 02/Ti6Al7Nb	3	250	143.05	92,21	7,79
I 212 04/Ti6Al7Nb	3	500	38.59	92,49	7,51
I 212 06/Ti6Al7Nb	3	1000	9.69	92,64	7,36
I31 02/Ti6Al7Nb	129	250	143.05	86,73	13,27
I31 04/Ti6Al7Nb	129	500	38.59	87,60	12,40
I31 06/Ti6Al7Nb	120	1000	9.69	87,62	12,38
Alloclassic 02/ Ti6Al7Nb	new	250	143.05	80,41	19,59
Alloclassic 04/Ti6Al7Nb	new	500	38.59	78,19	21,81
Alloclassic 06/Ti6Al7Nb	new	1000	9.69	89,47	10,53
Lima 02/Ti6Al4V	new	250	38.59	81,86	18,14
Lima 04/Ti6Al4V	new	500	9.69	83,93	16,07
Lima 06/Ti4Al4V	new	1000	1.55	82,62	17,38

3.2. The Estimation of Microstructure- Alpha and Beta Phase Contents in Ti6Al7Nb and Ti6Al4V Alloys

Ti implant alloys have a dual-phase microstructure (α + β). Their distribution was estimated using a field emission scanning electron microscope by SE (secondary electron image) and BE (backscattered electron image. Results are shown in Figure 4 and Table 2.

 doi:10.20944/preprints202405.0688.v1

The results of the microstructure analysis of selected retrieved and two new samples for comparison (Table 2) showed that according to the standards [32,33] (ASTM F-1295 Ti6Al7Nb; and ASTM F-136 Ti6Al4V), the dominant phase, α phase (matrix), with 85 to 92 % and 8 to 15% β Nb enriched phase of retrieved samples and 79 to 89 α phase and 11 to 21% of β phase of new samples of the same alloy Ti6Al7Nb. We compared microstructure analysis with Ti6Al4V alloy where we found 84% α phase, matrix, and V-enriched β phase 16%. Of all the investigated samples, only the I-212 stem taper that prematurely failed after 3 months due to infection hip endoprostheses differs slightly in microstructure with the lowest Nb enriched β phase. Besides the material properties, such as microstructure, the survivorship, of cementless is very complex and depends on several factors such as the impact on surgeons, the patient, materials, contamination, etc.

3.3. SEM/EBSD Characterization of Stem Taper Phase Microstructure

The quantitative determination of phase distributions in the new sample Ti6Al7Nb alloy is possible by using the electron-backscattered diffraction integrated technique on the field emission scanning electron microscope, EBSD, where the stem-taper microstructure is (α+β), Figure 5. The EBSD method is compatible with the XRD method, but on a smaller scale and for that reason is mounted on the FE-SEM. The EBSD method is very precise, the limitation of EBSD besides being a very accurate, precise method, is that it is very time consuming, and for that reason is suitable for basic research and development of new biomaterial alloys.

The microstructures of all the investigated stem tapers manufactured from Ti6Al7Nb alloy are similar. We compared the stem-tapers microstructure of Ti6Al4V and found that the latter is more small-grained which is already known from several investigations [17].

3.4. SEM / EDS Characterization of Stem-Taper New Implants Microstructure

Two new tapers were investigated for comparison with the retrieved, premature failed implants. The results were similar, so we represent one sample, with the longest survivorship A283 in Figure 7.

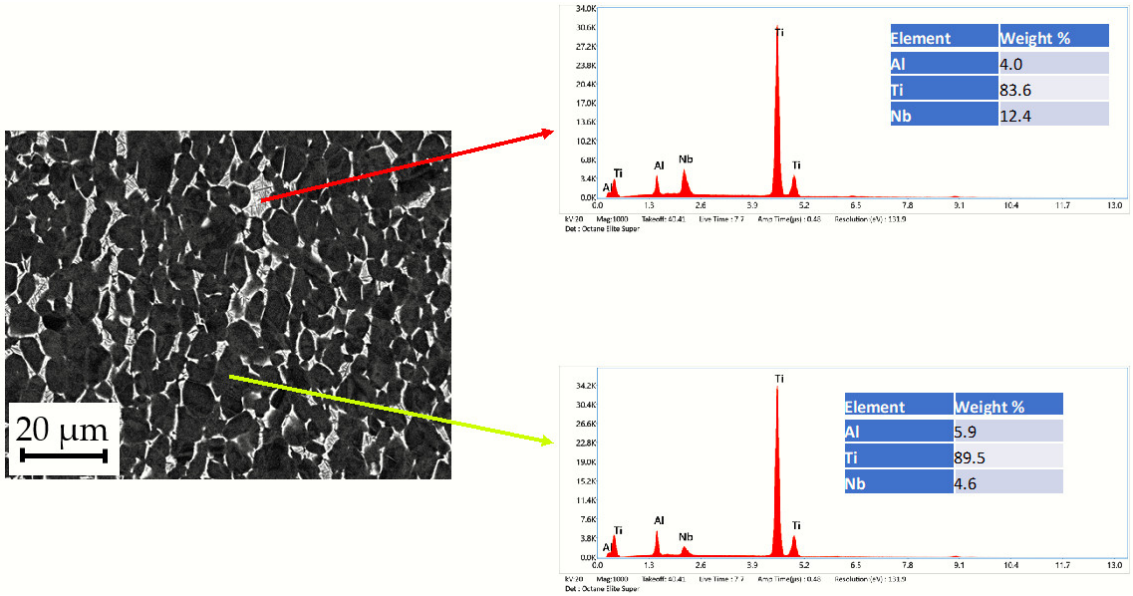

Figure 7. (a) SEM/BE image of A-283, Ti6Al7Nb alloy, stem-taper of the hip endoprosthesis, survivorship 239 months, aseptic loosening, microstructure dual phase is observed (b) Ti X-ray signal intensity, (c) Al X-ray signal intensity, (d) Nb X-ray signal intensity.

The SEM/EDS images of the surface chemistry are shown in Figure 7. The selected stem taper with a survivorship of 239 months, prematurely failed due to aseptic loosening. The typical (α + β) dual-phase Ti6Al7Nb alloy is shown in Figure 7 a. Figure 7 b shows the distribution of Ti in the sample, (c) EDS mapping shows the distribution of Al in the microstructure and (d) SEM/EDS

 doi:10.20944/preprints202405.0688.v1

mapping shows the distribution of Nb. We may conclude that the major dark grey phase is the Ti matrix, α-phase, and the light grey phase, enriched with Nb is the β-phase.

The images of the new, unused implants show some signs of abrasive damage and wear, which is attributed to the manufacturing process as seen in **Figure 8**. Some dark particles are visible in the backscattered electron images (BE), in the case of the Alloclassic implant (**Figure 8(b)**), while in the case of Lima Corporate implant taper, the surface seems rough, but no particles are visible in the (sub)surface area.

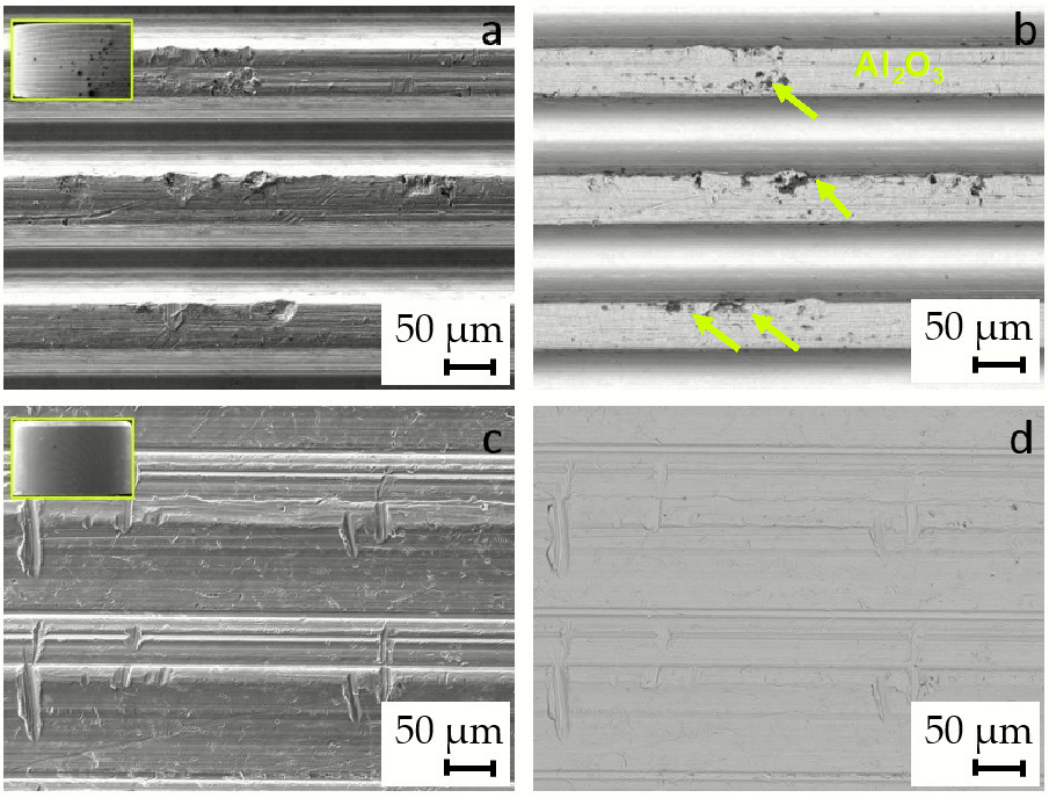

Figure 8. Images of the surface of the new, unused tapers. (a): SE image of Alloclassic new, (b) BE image of Alloclassic new; the remains of grit blasting are observed, dark particles, marked with yellow arrows, (c) SE image of Lima Corporate new, and (d) BE image of Lima Corporate new.

To identify the dark particles in the BE image of the Alloclassic taper part of the implant, we performed SEM/EDS mapping of a selected area. As is evident from the image in **Figure 9(b)**, the black particles are remnants of corundum (Al2O3) sandblasting that was performed as a finishing step in the taper manufacturing process. Additionally, the dual microstructure of the titanium alloy can be seen.

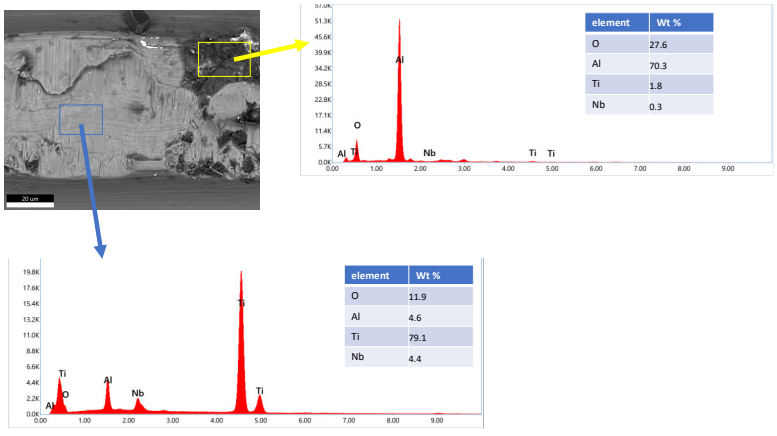

 doi:10.20944/preprints202405.0688.v1

Figure 9. EDS analysis of a selected area of new Alloclassic taper (a) BE image of the area, yellow box indicates the remnants of Al2O3(corundum) of micro threaded blaster finishing, blue box shows the matrix Ti6Al7Nb alloy.

On the other hand, the new implant Lima Corporate, does not show larger dark particles that are visible in the backscattered electron image. The surface of the new implant nonetheless shows signs of abrasive wear, as is evident from **Figure 10.**

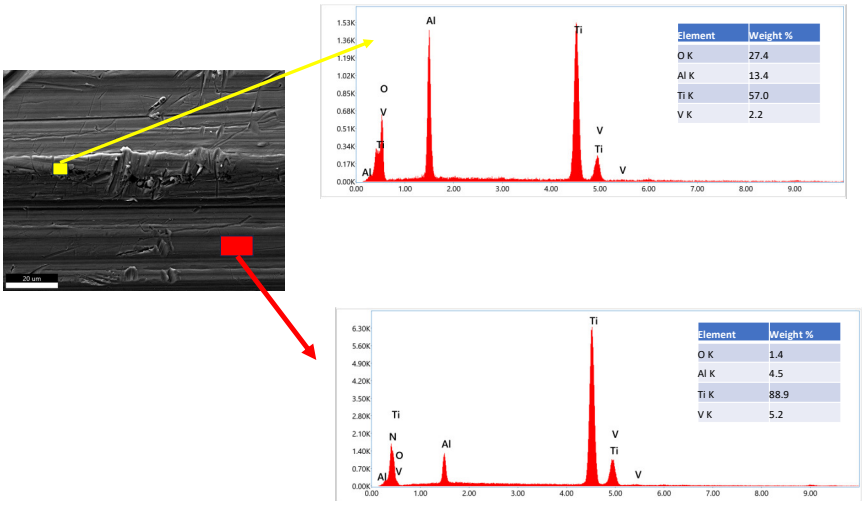

Figure 10. Surface damage (abrasive wear) of a new, unused Lima Corporate taper part of the implant. EDS mapping shows evidence of corundum Al_2O_3 particles implanted in the material due to the manufacturing process of the implant.

The new, unused tapers of the implants do not have a smooth surface, in both cases, and there is evidence of deposited material (Al2O3) from sandblasting, and mechanical wear damage is visible in both cases. It has been shown that corundum Al2O3 sandblasting remains from the process and affects the corrosion properties and can lead to an increased number of infections [11,12].

3.5. SEM /EDS Characterization of Prematurely Failed Implants

Three failed implants were chosen for examination with SEM/EDS. Two implants prematurely failed due to infection, the first one after 32 months and the second after 129 months, while the third implant failed because of aseptic loosening after 239 months. The images of the surfaces of the implant taper parts are shown in **Figure 11**.

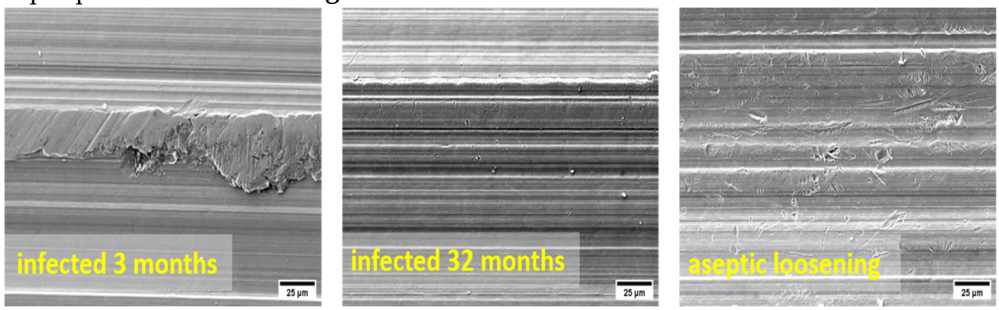

Figure 11. SE images of the surface of the three failed implants. The surface area shown in the figures is 230 μm x 170 μm.

The surfaces of prematurely failed implants show signs of abrasive wear, like the new, unused implants, mainly due to machining and further sandblasting, as seen in **Figure 12** and **Figure 13**. No cracks or oxidation products are visible on the implant surfaces. Additional abrasive wear (most prominent in the case of the implant that failed due to aseptic loosening) could also be attributed to the revision surgery.

 doi:10.20944/preprints202405.0688.v1

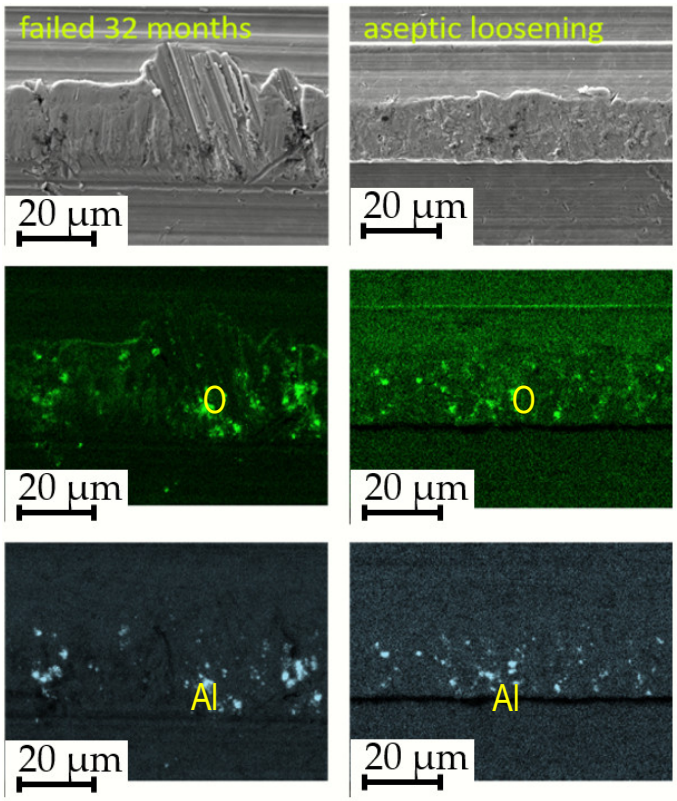

Figure 12. Evidence of corundum remains in an infected implant that failed after 32 months and an aseptically loosened implant after 239 months.

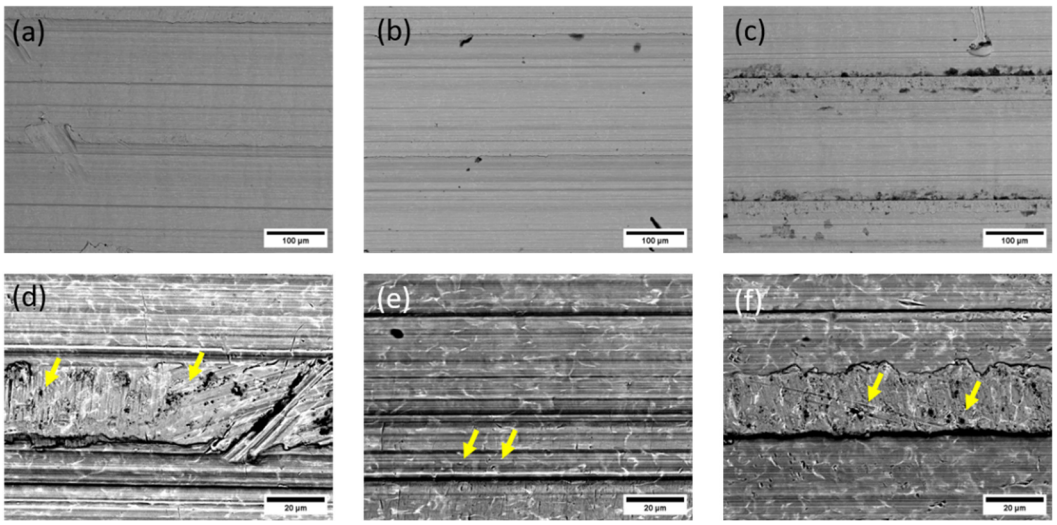

Figure 13. SEM/Backscattered electron images (BE) of the failed implant surfaces; (a) and (d) infected implant, failure time 3 months; (b) and (e) infected implant, failure -32 months; and (c) and (f) failure due to aseptic loosening after 239 months—the arrows in the lower panel point to locations of embedded corundum particle clusters.

EDS mapping showed that there are some remnants of corundum in the subsurface layers of the failed implants, as is seen in Figure 12. The corundum remains are clustered, and the particle sizes are up to approximately 10 µm in diameter, with a similar distribution compared to the new Lima implants. No large particles (such as in the case of a new Alloclassic implant) were found on the examined surfaces of the failed implants. This is most evident from large-scale backscattered electron images, shown in Figure 13, upper panel. Only at higher magnification (lower panel of Figure 13, it

Preprints.org (www.preprints.org) | NOT PEER-REVIEWED | Posted: 13 May 2024 doi:10.20944/preprints202405.0688.v1

is possible to distinguish individual clusters of small embedded corundum particles. In all implants, no signs of corrosion or cracks due to fretting were observed.

3.6. Stem Taper Morphology, Surface Roughness

Five samples were investigated, in Table 3, samples 1 to 5, two new (Alloclasic Varial -AV, and Lima corporate), and three retrieved (A-283, I-212, and I-031) with different survivorships from 3 to 239 months. Roughness profiles of stem tapers were obtained from the surface of the taper as seen in Figure 2. Peak spacing - s and profile depth – h (Figure 2c) also measured for comparison. As can be seen from Table 3, there is no significant difference in roughness associated with a longer time of use. New samples AV and Lima have the lowest and highest values of Ra and Rz values. Samples AV and Lima also have different profile depths of the peaks (Figure 2 c and 2d). Sample AV has an average depth of 9.3 and sample Lima 14.4 µm. (Table 3). This can be attributed to different manufacturers and thus different manufacturing methods. Retrieved samples on the other hand result in slightly lower values of surface roughness and profile depth which can contribute to the deformation of the peaks. Results of surface roughness indicate that the three retrieved samples (A-238, I-212, and I-031) were manufactured using the same or similar method as sample Lima.

Table 3. Roughness parameters Ra and Rz and profile depth and peak spacing for investigated new and retrieved samples.

	Ra [µm]	Rz [µm]	Profile depth[µm]	Peak spac. [µm]
A – new	1.98	9.64	206.3	9.3
B – new	2.92	14.90	209.7	14.4
C – 3 months	2.60	12.36	205.1	13.8
D – 13 months	2.27	13.22	199.9	14.1
E – 91 months	2.52	12.52	206.8	15.3

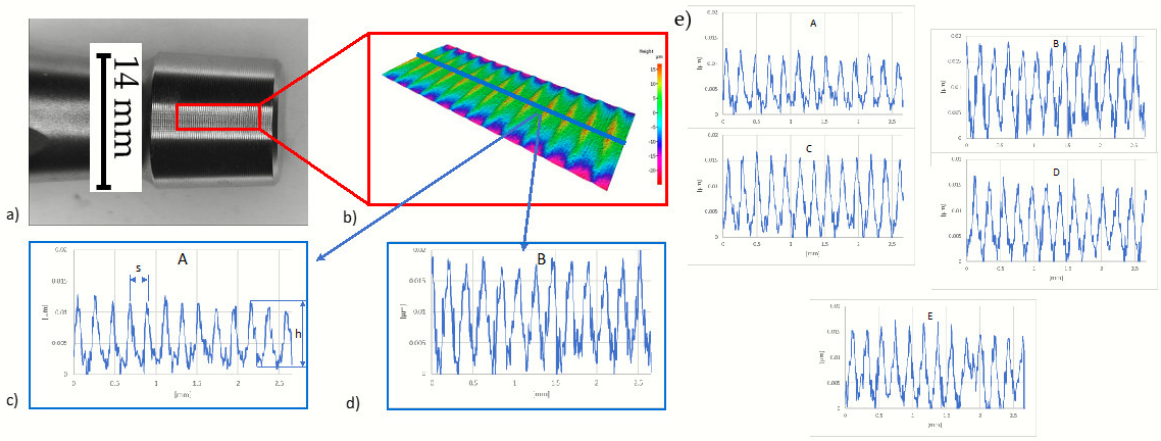

Figure 14. a) Image of male steam taper, b) 3D pseudo profile picture c) 2D roughness profile of stem A and d) 2D roughness profile of stem B, e) roughness of all five investigated stem tapers collected in Table 3.

3.7. Corrosion Properties of Investigated New and Retrieved Stem Taper Samples.

The potentiodynamic behaviour of the investigated materials in Hank's solution is shown in **Figure 15**. All the investigated materials exhibited a broad range of passivation after the Tafel region due to the formation of a compact outer passive film, which inhibits the diffusion of aggressive species and therefore improves the corrosion properties of the material [30,32,33]. The corrosion potentials (E_{corr}), corrosion current densities (i_{corr}) and corrosion rates (v_{corr}) are listed in **Table 4**. The results show that the corrosion rates for both the new samples and the one with the longest exposure to real-body conditions were lower compared to the other three with shorter exposure times. The implants with shorter exposure times to real-body conditions were all subjected to infection, which

 doi:10.20944/preprints202405.0688.v1

is probably related to the formation of conditions that are detrimental to corrosion. In contrast, new implants with an intact surface as well as the implant with the longest survival in real-body conditions showed an increased corrosion resistance.

Table 4. Electrochemical parameters determined from the potentiodynamic curves.

Material	E_{corr} (V)	i_{corr} (uA cm^{-2})	v_{corr} (um year^{-1})
I-212 surface-taper 32 months	-326,6	0,14	1,21
I-31 3 months	-250,7	0,14	1,20
A-283 239 months	-284,6	0,08	0,70
ALLOCLASSIC new	-286,3	0,09	0,81
LIMA Corporate new	-221,5	0,05	0,40

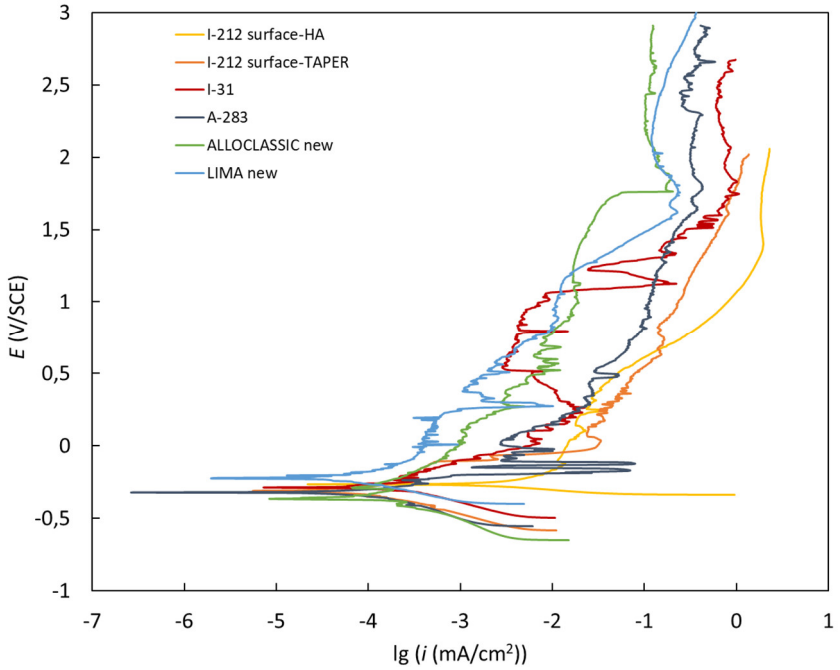

Figure 15. Potentiodynamic curves for the investigated new and retrieved samples were measured in simulated physiological Hank´s solution at pH=7.8 and 37 °C.

4. Discussion

This study investigated the damage that occurred in vivo on Ti-alloy micro-threaded 12/14 tapers. The in vivo damage in secondary implants with ceramic heads was compared with the new implants. Qualitative and quantitative evaluations were carried out on 45 retrievals.

Every modular connection of metal alloys in contact with body fluids and exposed to micromotion is subject to corrosion. The taper's interface is influenced by several factors, such as (i) design and material, (ii) assembly (surgical factors), and (iii) loading (patient factors).

Mueller et al. demonstrated that stem taper characteristics largely differ between manufacturers [4].

The assembly condition plays an important role in the strength of the taper's connection. Minimal invasive surgery with small incisions might indirectly be associated with the frequency of the taper's corrosion due to the challenges in cleaning the taper and applying appropriate assembly forces in the taper's direction.

We investigated retrievals provided by the Department for Orthopaedic Surgery of UMC Ljubljana, Slovenia in which the only source of modularity with a metallic component was the ceramic head stem-taper interface.

We investigated the corrosion resistance using electrochemical studies and there was no corrosion of the retrieved tapers that prematurely failed due to aseptic loosening after 239 months,

 doi:10.20944/preprints202405.0688.v1

infection after 3 months, and low-grade infection after 32 months. Further, three retrieved tapers and, for comparison, two new tapers were exposed to potentiodynamic measurements in Hank's solution. The results show very low corrosion rates for both new samples (Zimmer, Lima Corporate) and the retrieved sample that prematurely failed due to aseptic loosening after 239 months. The corrosion rates of the infected and low-grade infected tapers were higher. We observed small differences in the microstructure within the limits of the standards [17]. The microstructure is very important for minimizing corrosion and bio-tribo-corrosion, taper corrosion, etc., which can lead to aseptic loosening or joint infection, the main causes of failure with joint arthroplasty.

This study has some limitations. The ceramic femoral heads were not investigated in this study and no statement can be made about the material transfer from taper to ceramic head that can occur. However, Stockhausen reported that both fretting and corrosion scores in the head and the neck are correlated, making neck scores a good indicator of degradation in the head [2,3].

In our investigation we didn't observe taper corrosion, fretting, and crevice corrosion due to the use of ceramic heads with a dominant head size of 32 mm, which agrees with the published results [3,4,10] and the fact that the Slovenian hospital protocol requires carefully cleaned, rinsed, and dried taper stems before assembly.

Furthermore, corrosion of metal alloys always occurs in the human body due to the aggressive environment, but it does not necessarily become a clinical problem if the amount of corrosion is small. [4,34–41].

5. Conclusion

This study demonstrated that the 12/14 investigated tapers are not uniform, and the stem and head tapers are manufactured specifically in terms of geometry as well as topography at different manufacturers as well as from the same manufacturer.

In our study of different stems from prematurely failed cementless hip endoprostheses regarding the geometry, high variations in taper length were observed whereas the taper angle and opening taper diameter vary only to a small degree.

In our study we didn't observe taper corrosion, fretting, and crevice corrosion due to the use of ceramic heads with a dominant head size of 32 mm, which agrees with the published results and the fact that the hospital protocol requires carefully cleaned, rinsed, and dried taper stems before assembly.

Moreover, within the human body, metal alloys inevitably undergo corrosion owing to the hostile physiological environment. However, the clinical significance of this corrosion is not inevitable, contingent upon the extent of its occurrence.

Ultimately, the results from this study provide relevant taper design characteristics of new components, which can also serve as a reference for retrieval studies describing the initial state for experimental studies of taper corrosion.

It is obvious that further investigations of the influence of stem tapers of ZM cementless hip endoprostheses on the biological response are needed and the dimensions of the stem taper as well as materials are not standardized and vary between manufacturers. Therefore careful and precise assembly of the femoral component and ceramic acetabular heads is required/ very important.

Author Contributions: Conceptualization, M.J.; D.D., M.G.; B.K.; M.D.; B.S-B.; methodology, M.J.; D.D.; M.G.; A.K.; B.S-B.;.JTG, formal analysis, B.S-B; A.K.; investigation, M.G.; resources, M.J.; M.G., writing—original draft preparation, M.J.; M.D., writing—review and editing, M.D.; D.D.; M.G.; B.K., JTG supervision, D.D.; project administration, M.J., M.G. funding acquisition, M.J.and D.D., M.G. All authors have read and agreed to the published version of the manuscript.

Funding: This research was funded by the Slovenian Research Agency, ARIS, L3-2621, and the Department for Orthopedic Surgery UMC, Ljubljana, Slovenia, Tertiary projects: TP No. 20220103 and TP No. 20230194.

Conflicts of Interest: Declare conflicts of interest or state "The authors declare no conflict of interest."

References

1. Kurtz, S.; Ong, K.; Lau, E.; Mowat, F.; Halpern, M. Projections of primary and revision hip and knee arthroplasty in the United States from 2005 to 2030. J. Bone Joint Surg. Am. 2007, Volume 89, pp.780–785. *DOI:* 10.2106/JBJS.F.00222
2. Stockhausen, K.E.; Riedel., C.; Belinski, A.V.; Rothe, D.; Gehrke, T.; Klebig, F.; Gebauer, M.; Amling, M.; Citak, M.; Bussel, B. Variability in stem taper surface topography affects the degree of corrosion and fretting in total hip arthroplasty, Scientific Reports | (2021) 11:9348 | https://doi.org/10.1038/s41598-021-88234-3
3. Morlock, M.M.; Hube, R.; Wassilew, G.; Prange, F.; Huber, G.; Perka,C.; Taper corrosion: a complication of total hip arthroplasty, EOR, 2020, Volume 5, pp. 776-784. doi https://10.1302/2058-5241.5.200013
4. Mueller, U.; Braun, S.; Schroeder, S.; Sonntag,R.; J. Philippe Kretzer, J.P. Same Same but Different? 12/14 Stem and Head Tapers in Total Hip Arthroplasty, The Journal of Arthroplasty 2017, 32, 3191-3199. https://doi.org/10.1016/j.arth.2017.04.027
5. Cales,B.; Stefani, Y. Risks and advantages in standardization of bores and cones for heads in modular hip prostheses, Journal of Biomedical Materials Research, First published: 31 July 2002. https://doi.org/10.1002/(SICI)1097-4636(199821)43:1<62::AID-JBM7>3.0.CO;2-K
6. Martelli, A.; Erani, P.; Pazzagli, N.; Cannillo, V.; Baleani, M. Surface Analysis of Ti-Alloy. Micro-Grooved 12/14 Tapers Assembled to Non-Sleeved and Sleeved Ceramic Heads. A Comparative Study of Retrieved Hip Prostheses. Materials **2023,** 16, 1067. https://doi.org/10.3390/ma16031067
7. Merola, M., Affatato, S., Review Materials for Hip Prostheses. A Review of Wear and Loading Considerations. Materials 2019, Volume 12, pp. 495. doi:10.3390/ma12030495
8. Cör, A., Histological Picture of the Wear Particles, and the Biological Response in Periprosthetic Tissue, MTAEC9, 53(1)77(2019) doi:10.17222/mit.2018.160
9. Kocjančič B.; Avsec, K.; Šetina Batič, B.; Feizpour, D.; Godec, M.; Kralj-Iglič, V.; Podlipec, R.; Cör, A.; Debeljak, M.; Grant, J.T.; et al. The Impact of Al2O3 Particles from Grit-Blasted Ti6Al7Nb (Alloy) Implant Surfaces on Biocompatibility,Aseptic Loosening, and Infection. Materials 2023, 16, 6867. https://doi.org/10.3390/ma16216867
10. Jan, Z., Hočevar, M., Kononenko, V., Michelini, S., Repar, N., Caf, M., Kocjančič, B., Dolinar, D., Kralj, S., Makovec, D., Iglič, A., Drobne, D., Jenko, M., Kralj-Iglič, V. Inflammatory, oxidative stress and small cellular particle response in HUVEC induced by debris from endoprosthesis processing. *Materials*. 2023, vol. 16, iss. 9, str. 1-17, ilustr. ISSN 1996-1944. , doi: 10.3390/ma16093287.
11. Dolinar, D.; Gorenšek, M.; Jenko, M.; Godec, M.; Šetina, B.; Donik, Č.; Kocijan, A.,; Debeljak, M.; Kocjančič, B.; Biomaterials in endoprosthetics. Materiali in tehnologije, 2018, Volume 52, 1, pp. 89-9. doi: 10.17222/mit.2017.196
12. Savin, L.; Pinteala, T.; Mihai, D.N.; Mihailescu, D.; Miu, S.S.; Sirbu, M.T.; Veliceasa, B.; Popescu, D.C.; Sirbu, P.D.; Forna, N. Updates on Biomaterials Used in Total Hip Arthroplasty (THA). *Polymers* **2023**, *15*,3278. https://doi.org/ 10.3390/polym15153278
13. Jenko,M.; Gorenšek, M.; Godec,M.; Hodnik,M.; Setina Batic, B.; Donik, C.; Grant,J.T.; Dolinar, D. Surface chemistry and microstructure of metallic biomaterials for hip and knee endoprostheses. Applied Surface Science 2018, Volume 427A, pp. 584-593. doi.org/10.1016/j.apsusc.2017.08.007
14. Avsec, K.; Jenko, M.; Conradi,M.; Kocijan, A.; Vesel,A.; Kovač, J.; Godec, M.; Belič, I.; Šetina; B.; Donik, C.; Gorenšek, M.;, Kocjančič, B.; Dolinar,D. Surface properties of retrieved cementless femoral hip endoprostheses produced from a Ti6Al7Nb alloy. *Coatings*. 2019, Volume 9, 12, pp. 1-15. doi: 10.3390/coatings9120868
15. Urish,K.L, Giori,N.J., Lemons, J.E., Mihalko, W.M., Hallab,N. Trunnion corrosion in Total Hip Arthroplasty, Basics concepts, Orthop. Clin North Am. 2019 July 50(3):281-288 doi:10.1016/jocl.2019.02.001
16. Avsec, K.; Conradi, M.; Jenko, M.; Kocjančič, B.; Debeljak, M.; Gorenšek, M.; Dolinar, D. Effect of sterilization on the surface properties of Ti6Al7Nb alloy femoral stems Materiali in tehnologije 2021, Volume 55, 1, pp. 59-64. doi 10.17222/mit.2020.141.
17. Roškar, S.; Antolič, V.; Mavčič, B. Surgeon-stratified cohort analysis of 1976 cementless Zweymüller total hip arthroplasties from a single hospital with 23,255 component years of follow-up. Archives of orthopaedic and trauma surgery, 2020, Volume 140, pp. 1275-1283. doi: 10.1007/s00402-020-03517-0.
18. Soliman, M.M.; Chowdhury, M.E.H.; Islam, M.T.; Musharavati, F.; Mahmud, S.; Hafizh, M.; Ayari, M.A.; Khandakar, A.; Alam, M.K.; Nezhad, E.Z. Design and Performance Evaluation of a Novel Spiral Head-Stem Trunnion for Hip Implants Using Finite Element Analysis. Materials 2023, 16, 1466. https://doi.org/10.3390/ma16041466.
19. Urish,K.L, Giori,N.J., Lemons, J.E., Mihalko, W.M., Hallab,N. Trunnion corrosion in Total Hip Arthroplasty, Basics concepts, Orthop. Clin North Am. 2019 July 50(3):281-288 doi:10.1016/jocl.2019.02.001Cooper,J.; Della Valle, C. J. ; Berger R. A.; et al. Corrosion at the head-neck taper as a cause for adverse local tissue reactions after total hip arthroplasty. Journal of Bone and Joint Surgery—American Volume, 2012, Volume 94, 18, pp.1655–1661. doi: 10.2106/JBJS.K.01352.

20. Cooper,J.; Della Valle, C. J. ; Berger R. A.; et al. Corrosion at the head-neck taper as a cause for adverse local tissue reactions after total hip arthroplasty. Journal of Bone and Joint Surgery— American Volume, 2012, Volume 94, 18, pp.1655–1661. doi: 10.2106/JBJS.K.01352.
21. Godoy, M., Sipek, K., Gustafson, J.A.; Yuh, C.; Levine, B.R.; Pourzal,R.; Hannah J. Lundberg, H. J. Effect of Femoral Head Material, Surgeon Experience, and Assembly Technique on Simulated Head-Neck Total Hip Arthroplasty Impaction Forces, The Journal of Arthroplasty 2024, 39, 507-513 https://doi.org/10.1016/j.arth.2023.08.049.
22. Bitar, D.; Parvizi, J.; Biological response to prosthetic debris, World J. Orthop 6, 2015, Volume 2, pp. 172-189. doi: 10.5312/wjo.v6.i2.172.
23. Porter DA, Urban RM, Jacobs JJ, Gilbert JL, Rodriguez JA, Cooper HJ. Modern trunnions are more flexible: mechanical analysis of THA taper designs. Clin Orthop Relat Res 2014; Volume 472, pp. 3963–3970. DOI 10.1007/s11999-014-3965-3
24. C. Sittig,C.; Textor, M.; Spencer, N.D.; Wieland, M.; Vallotton P.H. Surface characterization of implant materials cp Ti, Ti-6Al-7Nb and Ti-6Al-4 V with different pretreatments. J. Mater. Sci. Med., 10 (1999), pp. 35-46. doi 10.1023/A:1008840026907
25. Raphel,J.; Holodniy, M.; Goodman, S.B. ; Heilshor, S.C. **Multifunctional coatings to simultaneously promote osseointegration and prevent infection of orthopaedic implants.** Biomaterials 2016, Volume 84 pp. 301-314.
26. doi: 10.1016/j.biomaterials.2016.01.016
27. ASTM G102 – 89 (2015) Standard Practice for Calculation of Corrosion Rates and Related Information from Electrochemical Measurements. Available online: https://www.astm.org/Standards/G102 (accessed on 10 February 2024).
28. Jauch SY, Coles LG, Ng LV, Miles AW, Gill HS. Low torque levels can initiate a removal of the passivation layer and cause fretting in modular hip stems. Med Eng Phys 2014; 36:1140–1146 http://dx.doi.org/10.1016/j.medengphy.2014.06.011.
29. ASTM F- 1295 Standard Ti6Al7Nb Standard Specification for Wrought Titanium-6Aluminum-7Niobium Alloy for Surgical Implant Applications (UNS R56700)
30. ASTM F-136 -13 (2021) Standard Ti6Al4V Standard Specification for Wrought Titanium-6Aluminum-4Vanadium ELI (Extra Low Interstitial) Alloy for Surgical Implant Applications (UNS R56401)
31. Lutzner J, Gunther KP, Postler A, Morlock M. Metal ion release after hip and knee arthroplasty - causes, biological effects, and diagnostics. *Z Orthop Unfall* 2020 Aug;158:369 382 https://doi.org/10.3390/diagnostics10110941
32. Del Balso C, Teeter MG, Tan SC, Howard JL, Lanting BA**.** Trunnionosis: does head size affect fretting and corrosion in total hip arthroplasty? *J Arthroplasty* 2016;31: 2332–2336. doi: 10.1302/0301-620x.97b7.35149
33. Osman K, Panagiotidou AP, Khan M, Blunn G, Haddad FS. Corrosion at the head-neck interface of current designs of modular femoral components: essential questions and answers relating to corrosion in modular head-neck junctions. *Bone Joint J* 2016;98– B:579–584. doi: 10.1302/0301-620x.98b5.35592
34. Kurtz, S. M. et al. Do ceramic femoral heads reduce taper fretting corrosion in hip arthroplasty? A retrieval study. *Clin. Orthop. Relat. Res.* **471**, 3270–3282 (2013). doi: 10.1007/s11999-013-3096-2
35. Kocagoz, S.B.; Underwood, R.J., MacDonald, D.W., Gilbert, J.L., S.M. Ceramic Heads Decrease Metal Release Caused by Head-taper Fretting and Corrosion. Clin Orthop Relat Res. 2016 Apr; 474(4): 985–994. doi: 10.1007/s11999-015-4683-1
36. Pezzotti, G. Affatato ,S.; Rondinella,A., Yorifuji M, Marin, E.; Zhu, W.; McEntire,B.; Bal, S.B.; Yamamoto,K., et al. In vitro versus in vivo phase instability of zirconia-toughened alumina femoral heads: a critical comparative assessment. *Materials (Basel).* 10, (2017). doi: 10.3390/ma10050466
37. Hallab, N.J. Fretting Corrosion of Orthopedic Implants**.** Comprehensive Biomaterials II, 2017 Volume 7, pp. 106-117.
38. Hothi, H.S.; Panagitopoulos A.C.; Whittaker, R.K.; Bills, P.J., McMillan, R.; Skinner,J.A.; Hart, A.J.; Damage patterns at the head-stem taper junction helps understand the mechanisms of material loss, The Journal of Arthroplasty 2017, Volume 32,291e295292. http://dx.doi.org/10.1016/j.arth.2016.06.045
39. Dyrkacz, R. M. R., Brandt, J.-M., Ojo, O. A., Turgeon, T. R. & Wyss, U. P. The influence of head size on corrosion and fretting behaviour at the head-neck interface of artificial hip joints. *J. Arthroplasty* **28**, 1036–1040 (2013). doi: 10.1016/j.arth.2012.10.017
40. Bechstedt, M. et al. Contact conditions for total hip head-neck modular taper junctions with micro-grooved stem tapers. *J. Biomech.* 109689 (2020).
41. Rehmer, A., Bishop, N. E. & Morlock, M. M. Influence of assembly procedure and material combination on the strength of the taper connection at the head-neck junction of modular hip endoprostheses. *Clin. Biomech. (Bristol, Avon)* **27**, 77–83 (2012).

 doi:10.20944/preprints202405.0688.v1